Analog Reflection Topology Building Blocks for Adaptive Microwave Signal Processing Applications

Stepan Lucyszyn, *Member, IEEE,* and Ian D. Robertson, *Member, IEEE*

Abstract—**The synthesis and realization of an analog—phase shifter, delay line, attenuator, and group delay synthesizer—are presented. These variable control devices are all implemented using the same generic single stage reflection topology. The optimum conditions of operation have been determined and the corresponding group delay behaviors have been investigated to produce simple design equations. As proof-of-concepts, monolithic technology has been used to realize an X-band, phase shifter, delay line, and attenuator. Hybrid technology has been used to realize an L-band, group-delay synthesizer. Because of the high levels of performance measured, these control devices are ideally suited for use as general building blocks in adaptive signal processing applications, including large phased array applications.**

I. Introduction

VARIABLE control devices play an important role in general adaptive signal processing applications. When compared to a purely digital implementation, analog control devices:

- require only one control wire per device
- do not require expensive foundry processing to realize high quality switches
- require almost no control power with a passive reflection topology incorporating varactor diodes and cold-FET's
- can make much more efficient use of expensive chip space with a reflection topology that uses active circulators [1]
- do not suffer from quantization errors
- easily correct for any degradation in performance attributed to fabrication process variations
- enable calibration corrections to be performed once integrated into a subsystem
- easily correct for any degradation in performance attributed to adverse operating conditions

As a result of these significant advantages, analog control devices appear ideal for large adaptive phased arrays and other high performance applications. The synthesis and realization of an analog—phase shifter, delay line, attenuator, and group delay synthesizer—are presented in this paper.

II. Synthesis

The design of the variable phase shifter (PS), delay line (DL), attenuator (AT), and group delay synthesizer (GDS) are all based on the same generic reflection topology, illustrated in Fig. 1. The table in Fig. 1 gives the reflection termination constraints for synthesizing the appropriate building block. For simplicity, the directional coupler is assumed to be lossless, perfectly matched, and having infinite isolation. With reference to Fig. 1, a proportion of the input power emerges from the direct port, where the resulting incident voltage wave is reflected from its terminating impedance, Z_T. A proportion of the reflected signal is transmitted back to the input port and a proportion is coupled into the isolated port. Similarly, the remainder of the input power emerges from the coupled port where its reflected signal is also sent to both the input and isolated ports. This scenario can be expressed analytically as follows:

$$S_{11} = \rho_T(S_{21}^{c2} + S_{41}^{c2}) \tag{1}$$

where S_{11} = input voltage reflection coefficient of the control device;ρ_T = voltage reflection coefficient of the reflection termination;S_{21}^c = coupled voltage transmission coefficient of the coupler; and S_{41}^c = direct voltage transmission coefficient of the coupler.

It can be seen from (1) that the voltage wave emerging from the input port will have zero amplitude when equal power split and phase quadrature, between the coupled and direct ports, are maintained—resulting in a perfect input and output impedance match. Also,

$$S_{21} = 2S_{21}^c\rho_T S_{41}^c \tag{2}$$

where S_{21} = forward voltage transmission coefficient of the control device.

It can be seen from (2) that the voltage wave emerging from the isolation port will have an amplitude equal to that entering the input port with a 3-dB directional coupler and purely reactive reflection terminations—resulting in zero insertion loss. From (2), the insertion phase of the control device is given by the following:

$$\angle S_{21} = \angle S_{21}^c + \angle\rho_T + \angle S_{41}^c. \tag{3}$$

Therefore,

$$\angle S_{21} = \angle\rho_T + 2\angle S_{41}^c + 90^\circ \text{when quadrature coupling is maintained} \tag{4}$$

and,

$$\angle S_{21} = \angle\rho_T + 90^\circ \cdot \left(1 - 2\frac{f}{f_0}\right) \text{with an ideal } \frac{\lambda}{4} \text{ transmission line coupler} \tag{5}$$

where,f = frequency and f_0 = center frequency.

Manuscript received May 9, 1994; revised July 13, 1994. This work was supported by the UK Engineering and Physical Sciences Research Council.

The authors are with the Communications Research Group, Department of Electronic and Electrical Engineering, King's College, University of London, Strand, London, WC2R2LS, England.

IEEE Log Number 9407449.

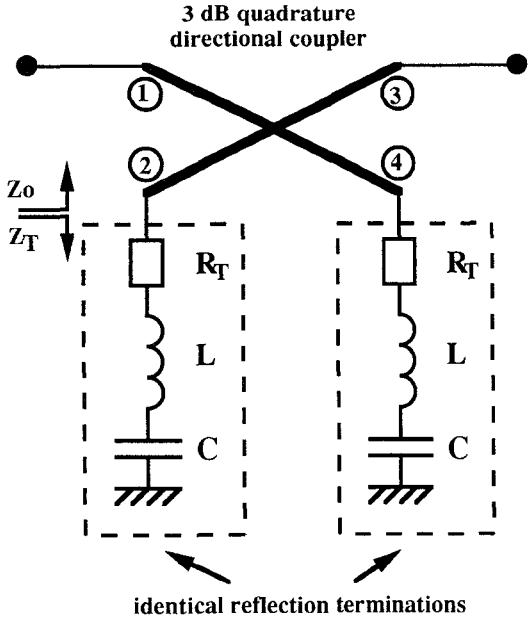

device \ variable	R_T	L	C
PS	0	0(*)	*(0)
DL	0	*	*
AT	*	0	0
GDS	*	*	*

* represents a positive value

Fig. 1. Generic reflection topology of the analog building blocks.

The voltage reflection coefficient of the reflection termination is expressed as follows:

$$\rho_T = \frac{Z_T - Z_O}{Z_T + Z_O} \tag{6}$$

$$Z_T = R_T + jX_T \tag{7}$$

Z_O = system reference impedance.

Therefore,

$$|\rho_T| = \sqrt{\left(\frac{R_T^2 - Z_O^2 + X_T^2}{(R_T + Z_O)^2 + X_T^2}\right)^2 + \left(\frac{2Z_O X_T}{(R_T + Z_O)^2 + X_T^2}\right)^2} \tag{8}$$

and,

$$\angle\rho_T = \tan^{-1}\left(\frac{2Z_O X_T}{R_T^2 - Z_O^2 + X_T^2}\right). \tag{9}$$

Now, the group delay of the control device, τ, is defined by the following expression:

$$\tau = -\frac{\partial\angle S_{21}}{\partial\omega} \tag{10}$$

where ω = angular frequency. Therefore,

$$\tau = \tau_{\min} - \frac{\partial\angle\rho_T}{\partial\omega} \tag{11}$$

where

$$\tau_{\min} = \frac{\pi}{\omega_O} \text{ dictated by the ideal } \frac{\lambda}{4} \text{ directional coupler} \tag{12}$$

and, for a general lossy series tuned circuit reflection termination,

$$\frac{\partial\angle\rho_T}{\partial\omega} = -\frac{2Z_O(X_L - X_C)}{\omega} \cdot \left(\frac{2X_T^2 - (R_T^2 - Z_O^2 + X_T^2)}{(2Z_O X_T)^2 + (R_T^2 - Z_O^2 + X_T^2)^2}\right) \tag{13}$$

$$X_T = X_L + X_C \tag{14}$$

$$X_L = \omega L \text{ i.e. reactance of inductance } L \tag{15}$$

$$X_C = \frac{-1}{\omega C} \text{ i.e. reactance of capacitance } C \tag{16}$$

A. Phase Shifter

An ideal phase shifter can be defined as a control device that has a constant group-delay frequency response, that does not change as its insertion phase varies, within its defined bandwidth of operation. Its two characteristics features are: a flat relative phase-shift frequency response, at all levels of relative phase shift; and no change in the timing of an input RF pulse envelope. As a result, ideal phase shifters can be employed in multiple space diversity receiver-combiners for aligning RF signals within a pulse envelope, but, without changing the timing of the pulse edges. However, they should not be employed in wideband beam forming networks for large aperture phased array antennas, in order to avoid the effects of 'phase squinting' and 'pulse stretching'.

To implement a true wideband analog phase shifter with a low phase error performance and constant group delay, a two-stage cascaded-match reflection-type phase shifter is required [2]. However, the more traditional single stage reflection topology [3], [4], shown in Fig. 1, is not an ideal phase shifter, since the phase error performance is usually very poor across wide frequency ranges. As a result, group delay can vary significantly for different levels of relative phase shift. It will be demonstrated that a Lange coupler with capacitive reflection terminations can have a level of phase error that is proportional

to bandwidth. Therefore, an extremely small phase error can be achieved across a narrow bandwidth. The conditions required to achieve this optimal bandwidth, for a specified level of absolute maximum phase error, will be presented. For the simplified case of a lossless single reactive element reflection termination:

$$\frac{\partial \angle \rho_T}{\partial \omega} = -\frac{2Z_O|X_T|}{\omega(X_T^2 + Zo^2)}. \tag{17}$$

At center frequency, as the reactance varies from either $|X_T| = 0$ or ∞ towards $|X_T| = Zo$ the insertion phase gradient will decrease and, therefore, the group delay will increase. In practice, a variable single reactive element can be implemented with either varactor diodes [5]–[7] or through the use of tunable active inductors (TAIs) [8], [9].

Equation (17) can be re-written as follows:

$$\frac{\partial \angle \rho_T}{\partial \omega} = -\frac{\tau_T(0)}{1 + \left(\frac{\omega}{\omega_c}\right)^2} \tag{18}$$

where,

$$\tau_T(0) = 2CZo\left(\text{or } \frac{2L}{Zo} \text{ for an inductor}\right) \tag{19}$$

and,

$$\omega_c = \frac{1}{CZo}\left(\text{or } \frac{Zo}{L} \text{ for an inductor}\right). \tag{20}$$

From (18), it can be deduced that the frequency response of the group delay will resemble the insertion loss frequency response of a varying first order Butterworth low pass filter and, therefore, be nonlinear. It has been found that the Lange coupler approximates an ideal 3-dB quadrature coupler at center frequency. Therefore, accurate predictions of the relative phase shift and the variation in group delay can be made at center frequency. The reduction in the coupling coefficient, away from center frequency, has been exploited to compensate for the nonlinear behavior of the group delay frequency response. As a result, the group-delay frequency response can be considered constant, as a first order approximation within a 40% bandwidth, BW_{lin}, centred on f_o—for any value of reflection termination capacitance or inductance. The resulting ideal insertion phase frequency response of the phase shifter with an ideal Lange coupler is illustrated in Fig. 2. It can be seen that the maximum relative phase shift, $\Delta\angle S_{21}|_{\max}$, will always be less than 180° for a single reactive element reflection termination.

By inspection of Fig. 2, the worst-case bandwidth scenario, which also gives the maximum variation in group delay, will occur when $|X_T|$ is either always below Zo or always above Zo. With the absolute maximum tolerable phase error, $\delta_{\text{abs. max}}$, it can be shown that the maximum bandwidth of operation, $\text{BW}_{\max}$, for this worst-case scenario can be expressed as follows: for $0 \le \Delta\angle S_{21}(\omega_o)|_{\max} \le 90°$:

$$\frac{BW_{\max}}{f_o} = \frac{2|\delta|_{\text{abs. max}}}{\Delta\angle S_{21}(\omega_o)|_{\max}} \tag{21}$$

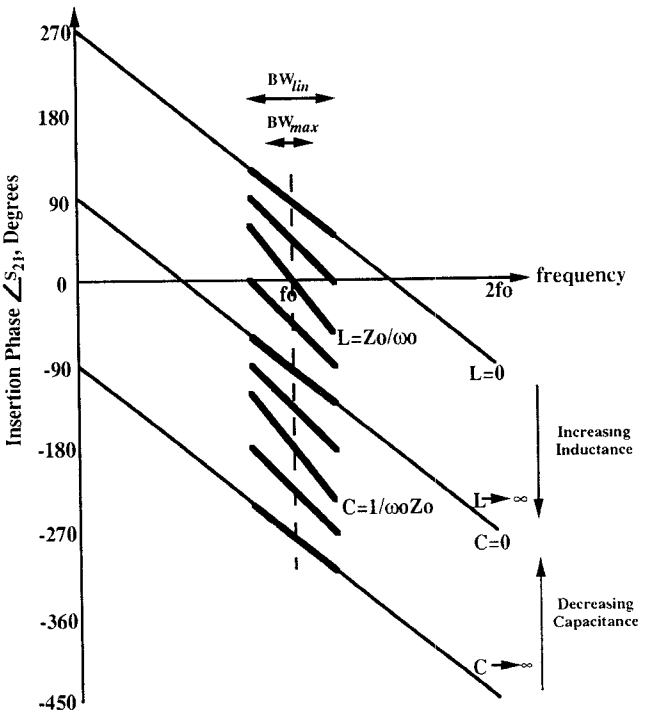

Fig. 2. Ideal insertion phase frequency responses of the phase shifter.

for $90° \le \Delta\angle S_{21}(\omega_o)|_{\max} \le 180°$:

$$\frac{BW_{\max}}{f_o} = \frac{|\delta|_{\text{abs. max}}}{45°}. \tag{22}$$

The optimum conditions of operation will now be investigated for the design of a phase shifter with single reactive element reflection terminations having either a minimum variation in group delay or a maximum relative phase shift—for a fixed value of $\delta_{\text{abs. max}}$.

B. Minimum Group Delay Variation

If the fractional relative phase shift at center frequency is given by

$$\alpha = \frac{\Delta\angle S_{21}(\omega_o)}{\Delta\angle S_{21}(\omega_o)|_{\max}} \tag{23}$$

the *minimum group delay variation* condition is achieved when the maximum group delay at center frequency, τ^+, occurs at $\alpha = 0.5$. The resulting maximum fractional bandwidth of operation for this best-case scenario can be expressed as follows: for $0 \le \Delta\angle S_{21}(\omega_o)|_{\max} \le 180°$:

$$\frac{BW_{\max}}{f_o} = \frac{4|\delta|_{\text{abs. max}}}{\Delta\angle S_{21}(\omega_o)|_{\max}}. \tag{24}$$

This expression shows that bandwidth is inversely proportional to the maximum level of relative phase shift. Using (24) it can be shown that with the *minimum group delay variation* condition the maximum phase error, $\delta_{\max}$, within $\text{BW}_{\max}$ is given by the following:

$$\psi = \Delta\angle S_{21}(\omega_o)|_{\max} \cdot \left(\frac{BW_{\max}}{f_o}\right) \tag{25}$$

for $0 \leq \alpha \leq 0.5$:

$$|\delta|_{\max} = \alpha \cdot \left(\frac{\psi}{2}\right) \tag{26}$$

and for $0.5 \leq \alpha \leq 1.0$:

$$|\delta|_{\max} = (1-\alpha) \cdot \left(\frac{\psi}{2}\right). \tag{27}$$

It has been found that when operating in this best-case bandwidth scenario, the group delay and its peak variation at center frequency, σ, can be accurately predicted from the following:

$$\tau = \tau^{\circ} + 2|\sigma| \sin(\alpha 180^{\circ}) \tag{28}$$

where,

$$\sigma = \pm\left(\frac{\tau^{+} - \tau^{\circ}}{2}\right) \tag{29}$$

$$\tau^{+} = \frac{1+\pi}{\omega_o} \tag{30}$$

and,

$$\tau^{\circ} = \tau_{\min} + \xi \cos(0.5\Delta\angle S_{21}(\omega_o)|_{\max}) \tag{31}$$

$$\xi = \frac{1}{\omega_o}. \tag{32}$$

For the *minimum group delay variation* condition, the ideal group delay variation at centre frequency and the corresponding maximum phase error within, $BW_{\max}$, are illustrated in Fig. 3, for variations in fractional relative phase shift. Using (12), (17), (31), simple design equations for the minimum and maximum reactance values and the associated frequency tuning ratio, m, of the reflection terminations can be determined as follows:

$$(\tau - \tau_{\min}) \equiv -\left.\frac{\partial\angle\rho_T}{\partial\omega}\right|_{\omega_o} \tag{33}$$

with,

$$\tau \equiv \tau^{\circ}. \tag{34}$$

Therefore, for a lossless single reactive element reflection termination,

$$|X_T| = \frac{1 \pm \sqrt{1-(2\gamma Zo)^2}}{2\gamma} \tag{35}$$

where

$$\gamma = \frac{\omega_o\tau - \pi}{2Zo}. \tag{36}$$

Therefore,

$$m = \sqrt{\frac{|X_T|_{\max}}{|X_T|_{\min}}}. \tag{37}$$

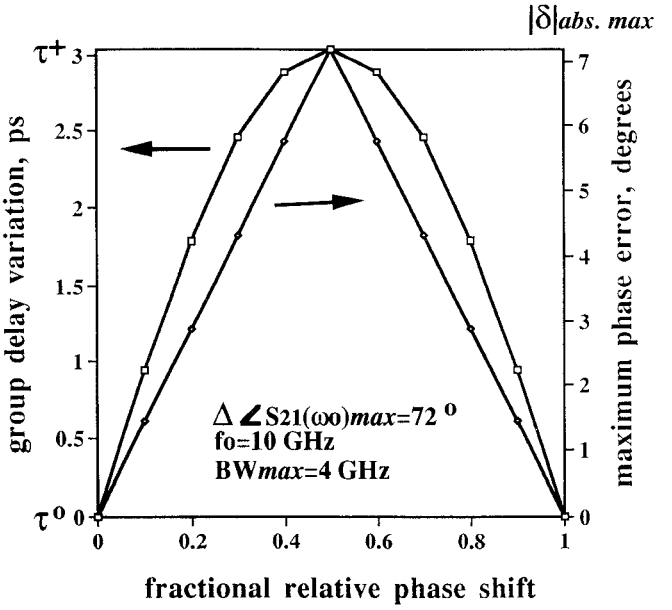

Fig. 3. Phase shifter characteristics when operating in the minimum group delay variation condition.

The minimum and maximum values for capacitance or inductance can be obtained from $|X_T|$ using (15) or (16). For an MMIC implementation, standard MESFET's can be used to realize practical interdigitated planar Schottky varactor diodes (IPSVDs). Using this low cost technique, it has been demonstrated that the zero bias junction capacitance values can range from 0.1 to 10 pF [7]—while having a frequency tuning ratio of approximately 2.6 [6]—using standard GaAs foundry processing. If, however, optimal IPSVD topographies and processing are employed frequency tuning ratios in excess of 7.5 can be achieved [5]. A TAI, realized using low cost foundry processing techniques, has been reported with a frequency tuning ratio of 4.5 [8].

C. Maximum Relative Phase Shift

For some applications the maximum level of relative phase shift attainable with a single stage topology is of primary importance. It has been found that $\Delta\angle S_{21}(\omega_o)|_{\max}$ can be increased by 25% for the same maximum bandwidth obtained when operating in the previous minimum group delay variation condition. Alternatively, the maximum bandwidth can be increased by 25% for the same value of $\Delta\angle S_{21}(\omega_o)|_{\max}$. For this *maximum relative phase shift* condition, $\Delta\angle S_{21}(\omega_o)|_{\max}$ has a reduction in its upper theoretical limit to 150°. The resulting maximum bandwidth of operation for this new best-case scenario can be expressed as follows: for $0 \leq \Delta\angle S_{21}(\omega_o)|_{\max} \leq 150°$:

$$\frac{BW_{\max}}{f_o} = \frac{5|\delta|_{\text{abs. max}}}{\Delta\angle S_{21}(\omega_o)|_{\max}}. \tag{38}$$

A typical example of the fractional bandwidth performance curves for the worst- and best-case scenarios is illustrated in Fig. 4, with $\delta_{\text{abs. max}} = \pm 5°$. While providing the largest maximum bandwidth, the penalty for this new operating condition is a doubling in the peak variation in group delay

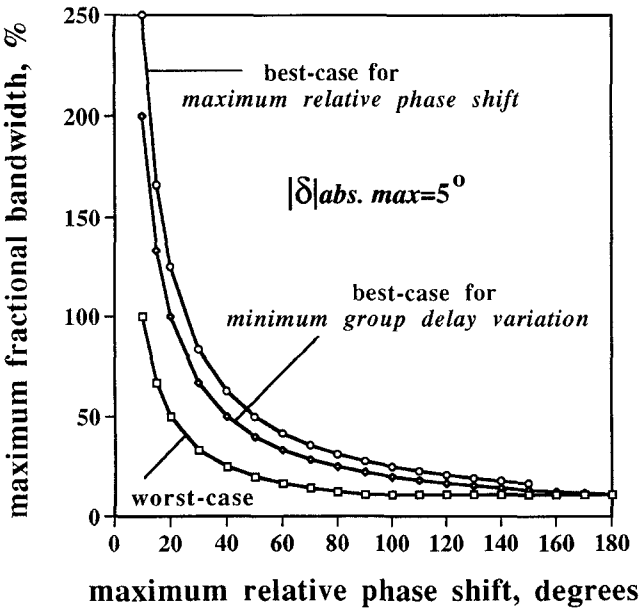

Fig. 4. Bandwidth performance of the phase shifter for different operation scenarios.

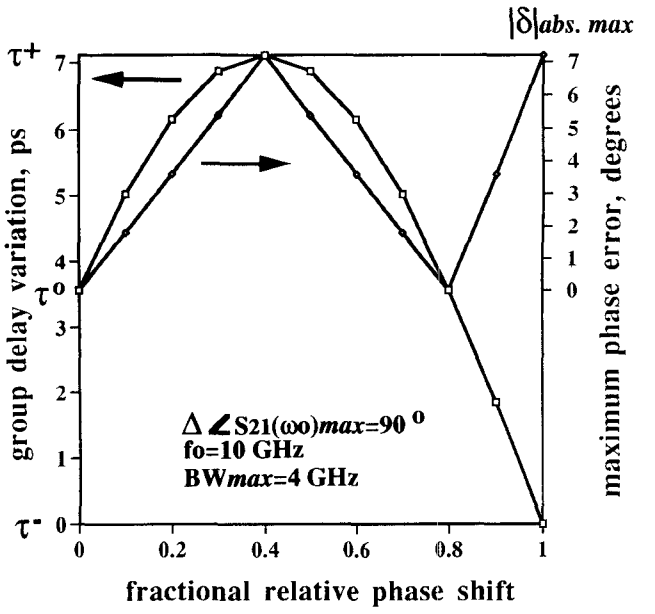

Fig. 5. Phase shifter characteristics when operating in the maximum relative phase shift condition.

at center frequency and an increase in the required frequency tuning ratio. Using (38) it can be shown that with the *maximum relative phase shift* condition the maximum phase error, $\delta_{\max}$, within $\mathrm{BW}_{\max}$ is given by the following: for $0 \leq \alpha \leq 0.4$:

$$|\delta|_{\max} = \alpha \cdot \left(\frac{\psi}{2}\right) \tag{39}$$

for $0.4 \leq \alpha \leq 0.8$:

$$|\delta|_{\max} = (0.8 - \alpha) \cdot \left(\frac{\psi}{2}\right) \tag{40}$$

for $0.8 \leq \alpha \leq 1$:

$$|\delta|_{\max} = (\alpha - 0.8) \cdot \psi. \tag{41}$$

It has been found that when operating in this new best-case bandwidth scenario, the group delay and its peak variation at center frequency can be accurately predicted from the following:

$$\tau = \tau^- + 2|\sigma| \sin(30° + \alpha 150°) \tag{42}$$

where,

$$\sigma = \pm(\tau^\circ - \tau^-) \tag{43}$$

$$\tau^\circ = \tau_{\min} + \xi \cos(0.4\Delta\angle S_{21}(\omega_o)|_{\max}) \tag{44}$$

and,

$$\tau^- = \tau_{\min} + \xi \cos(0.6\Delta\angle S_{21}(\omega_o)|_{\max}). \tag{45}$$

For the maximum relative phase shift condition, the ideal group delay variation at centre frequency and the corresponding maximum phase error, within $\mathrm{BW}_{\max}$, are illustrated in Fig. 5, for variations in fractional relative phase shift. Simple design equations for the minimum and maximum reactance values can be determined using (33), (35), and (36), where the minimum value of $|X_T|$ is determined with

$$\tau \equiv \tau^\circ \qquad \text{for } |X_T| \leq Zo \tag{46}$$

and, the maximum value of $|X_T|$ is determined with,

$$\tau \equiv \tau^- \qquad \text{for } |X_T| \geq Zo. \tag{47}$$

In the same way as before, the minimum and maximum values for capacitance or inductance, and the corresponding frequency tuning ratio, can be obtained from $|X_T|$, using (15) or (16) and (37).

D. Delay Line

An ideal time shifter can be defined as a control device that has a constant group delay frequency response with a level that changes as its insertion phase varies, within a defined bandwidth of operation. Its two characteristic features are: a linear relative phase shift frequency response, with a gradient that changes as the value of relative phase shift varies; and a change in the timing of an input RF pulse envelope. A special case of an ideal time shifter is a variable delay line, which is defined by the following:

$$\Delta\tau = \frac{\Delta\angle S_{21}(\omega)}{\omega} \tag{48}$$

where $\Delta\tau$ = relative shift in group delay.

Therefore, the group delay for a true delay line can be expressed as follows:

$$\tau = \tau_{\max} - \alpha\Delta\tau|_{\max} \tag{49}$$

where,

$$\Delta\tau|_{\max} = \frac{\Delta\angle S_{21}|_{\max}}{\omega}. \tag{50}$$

Therefore, using (23),

$$\tau = \tau_{\max} - \frac{1}{f} \cdot \left(\frac{\Delta\angle S_{21}}{360°}\right). \tag{51}$$

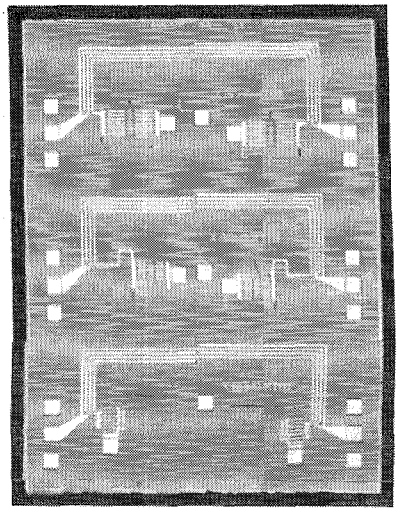

(a)

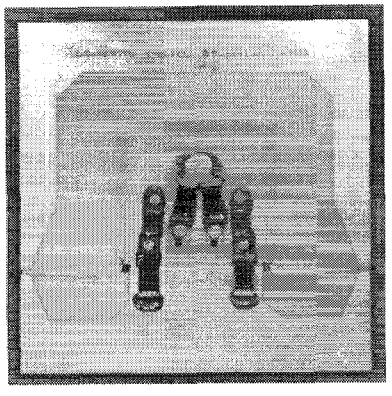

(b)

Fig. 6. Building block implementations: (a) monolithic phase shifter, delay line and attenuator; (b) hybrid group delay synthesizer.

Variable delay lines are required in adaptive beam forming networks of wideband phased array antennas. For large aperture arrays, containing hundreds or thousands of elements, the delay lines should ideally have the following characteristics:

- at the lowest frequency of operation, ω_1, $\Delta\angle S_{21}(\omega_1)|_{\max} = 360°$
- large number of phase states, with high accuracy
- $\Delta\tau = (\Delta\angle S_{21})/\omega$, at all operational frequencies
- negligible PM/AM conversion
- very low insertion loss
- very high return loss
- very low control power

Common classes of general time shifters that are compatible with both hybrid and monolithic microwave integrated circuit technologies are: switched-line [10]; loaded-line [11]; and reflection-type [12]. With the switched-line approach, PIN diodes or switching MESFET's are employed to route the input RF signal into the appropriate length of matched transmission line. The amount of induced group delay is directly proportional to the difference in the physical lengths of the selected line and the reference line. With this purely digital implementation, a wide bandwidth can be achieved, however, the amount of chip space increases exponentially as the required number of phase states increases. With the loaded-line approach, a transmission line is periodically loaded with shunt reactive elements to ground. The amount of induced group delay increases with an increase in shunt element capacitance. In order to mutually cancel the reflections from theses elements, they have to be separated by a $\lambda/4$ section of line and the induced phase shift per section must be small. This usually analog implementation is essentially narrow band and still requires considerable chip space. Until recently, only digital reflection-type time shifters had been reported [12]. Here, identical lumped element tapped transmission lines terminate the coupled and direct ports of the directional coupler. A number of equally spaced shunt switches can connect the transmission line to ground, but, only one switch per reflection termination is in the on-state at any time. Ideally, the amount of induced group delay is directly proportional to the distance along the line from the on-state switch to the reference off-state switch. While providing a wide bandwidth and requiring only minimal chip space, there is a practical limit on the number of possible phase states at higher microwave frequencies—due to the physical size of the switches. Also, where power is at a premium, as in the case of satellite or portable applications, considerable control power would be required for large aperture arrays.

It can be deduced from Fig. 2 that the reflection-type phase shifter having a single reactive element reflection termination, operating in the worst-case bandwidth scenario, can exhibit a time shifter characteristic. However, a true delay line characteristic can only be exhibited over a very narrow frequency range. In order to achieve a wideband performance, it has been found that the reflection terminations must consist of a variable capacitor in series with a fixed inductor. The first proof-of-concept analog reflection-type delay line, employing a Lange coupler, was demonstrated using hybrid technology [13]. Here, the center frequency was 750 MHz and a high performance was measured over a 40% bandwidth. No analysis of this analog delay line was presented.

Now, (13) can be re-written for a lossless series L-C tuned circuit in the following form:

$$\frac{\partial\angle\rho_T}{\partial\omega} = -\tau_T(0) \cdot \frac{\left(\frac{\omega}{\omega_{os}}\right)^2 = 1}{\left(\frac{\omega}{\omega_{os}}\right)^4 + 2\left(\frac{\tau_T(0)}{\tau_T(\omega_{os})} + 1\right)\left(\frac{\omega}{\omega_{os}}\right)^2 + 1} \tag{52}$$

where,

$$\tau_T(0) = 2CZo \tag{53}$$

$$\tau_T(0) = \frac{4L}{Zo} \tag{54}$$

and,

$$\omega_{os} = \frac{1}{\sqrt{LC}}. \tag{55}$$

From (52), it can be deduced that the frequency response of the group delay will resemble the insertion loss response of a

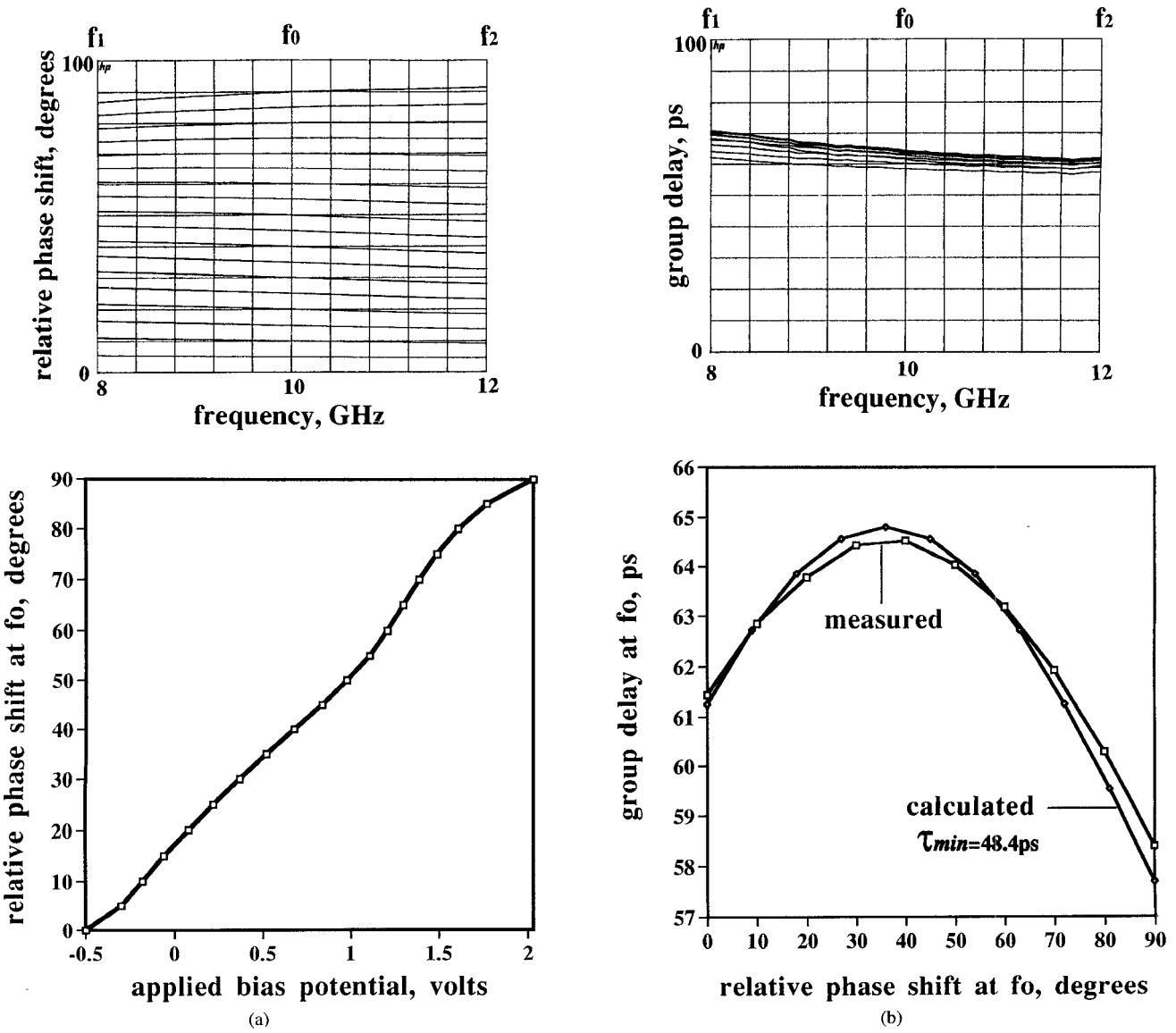

Fig. 7. Measured performance of the phase shifter: (a) relative phase shift; (b) group delay.

second order low pass filter and, therefore, be highly nonlinear. As with the phase shifter, a Lange coupler has been used to compensate for the nonlinear behavior of the group delay frequency response. The resulting design equations for a true variable delay line, employing a four-finger Lange coupler, have been determined empirically and are given below:

$$L = \frac{4.0}{f_o} nH; \quad C_{\max} = \frac{3.0}{f_o} pF; \quad \text{and} \quad R_T \leq \frac{Zo}{10}\Omega \tag{56}$$

where, f_o has units of GHz.

From (3), it is clear that the relative phase shift is equal to the amount of change in the angle of the voltage reflection coefficient of the reflection termination, when an ideal coupler is employed. Therefore, as a good approximation, the frequency tuning ratio required by the variable capacitor can be determined from the following: for $\omega_1 \leq \omega \leq \omega_2$:

$$m = \frac{1}{1 - \dfrac{\Delta\angle S_{21}(\omega)|_{\max}}{180^\circ} \cdot \left(\dfrac{\omega_{os}|_{\min}}{\omega}\right)} \tag{57}$$

where

$$\omega_{os}|_{\min} = \frac{1}{\sqrt{LC_{\max}}}. \tag{58}$$

E. Attenuator

Variable attenuators are control devices traditionally found in vector modulators, adaptive beam forming networks and measurement set-ups. In addition, they can be used as variable taps, in direct implementation transversal and recursive filter architectures. An analog reflection-type attenuator topology was demonstrated by Devlin [14]. Here, a resistive reflection

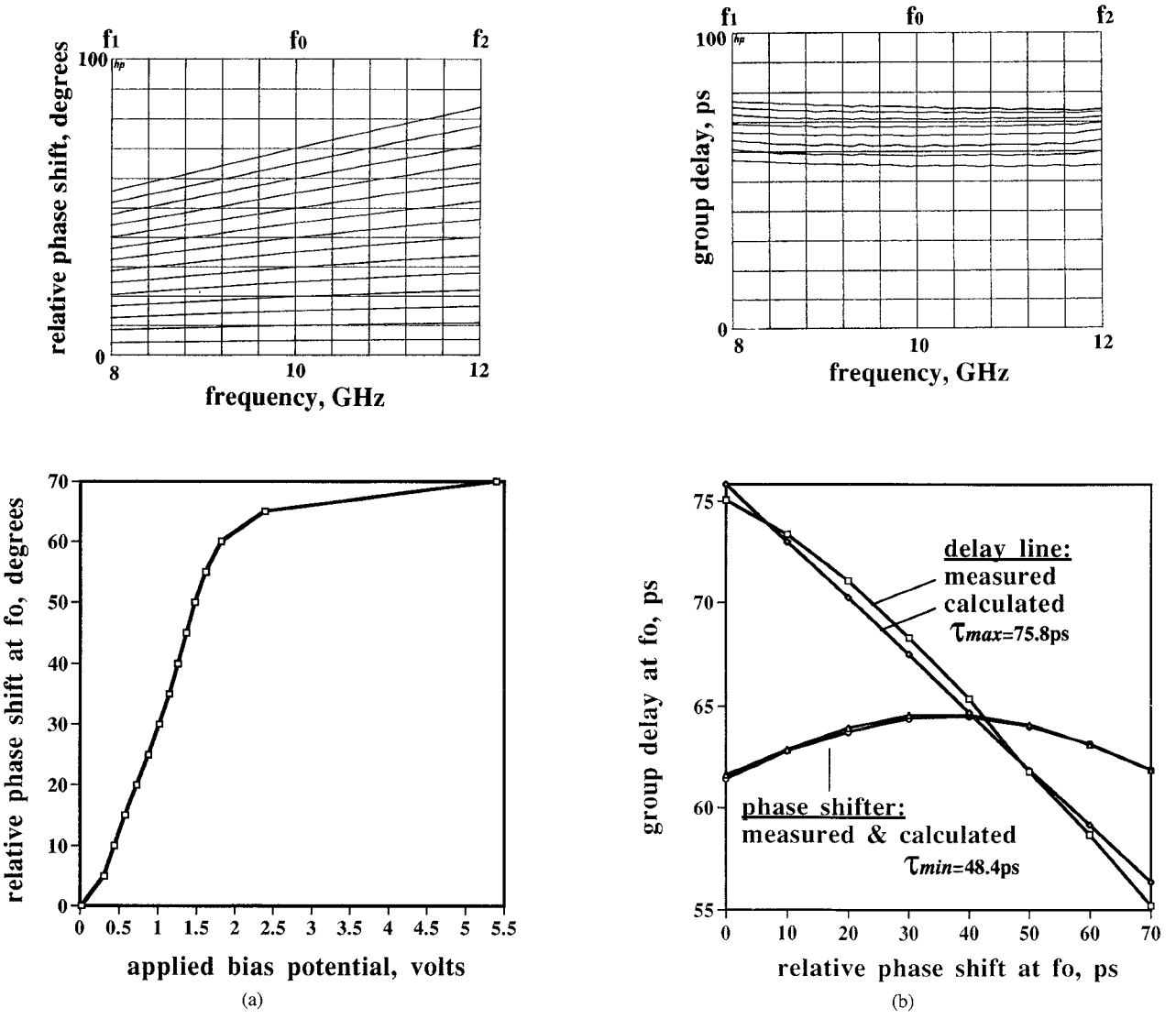

Fig. 8. Measured performance of the delay line: (a) relative phase shift; (b) group delay.

termination was realized with a cold-FET. Unfortunately, no measured results were reported for this device. The measured performance for a similar analog reflection-type attenuator is given in this paper.

F. Group Delay Synthesizer

A variable group delay synthesizer is a control device that traditionally finds applications in adaptive group delay equalization networks. By inspection of (10), it is apparent that the negative insertion phase gradient will result in a positive group delay, and a positive gradient can result in a negative group delay.

It has been found that with a reflection topology employing simple R-L-C tuned circuit reflection terminations, both positive and negative gradients can be achieved. Using (11), (13), it can be shown that when series resonance occurs at center frequency

$$\tau|_{\omega_{os}} = \tau_{\min} + \tau_T(\omega_{os}) \tag{59}$$

where

$$\tau_T(\omega_{os}) = \frac{4ZoL}{Zo^2 - R_T^2}. \tag{60}$$

From (60), it can be deduced that as the series resistance of the reflection termination increases from $R_T = 0$ towards Zo^-, the group delay will rapidly increase from $\tau|_{\omega_{os}} = (\tau_{\min} + 4L/Zo)$ towards $+\infty$. Similarly, if the resistance decreases from $R_T = \infty$ towards Zo^+, the group delay will rapidly decrease from $\tau_{\min}$ towards $-\infty$. It must be noted that when the network is lossy, the group delay of a network is not the same as the transit time through the network. Therefore, when synthesizing large positive or negative group delays, a significant insertion loss penalty will be incurred.

III. Realization

As proof-of-concepts, monolithic technology has been used to realize an X-band: phase shifter; delay line and attenuator. These control devices were designed using the equations presented in this paper for a center frequency of 10 GHz and a

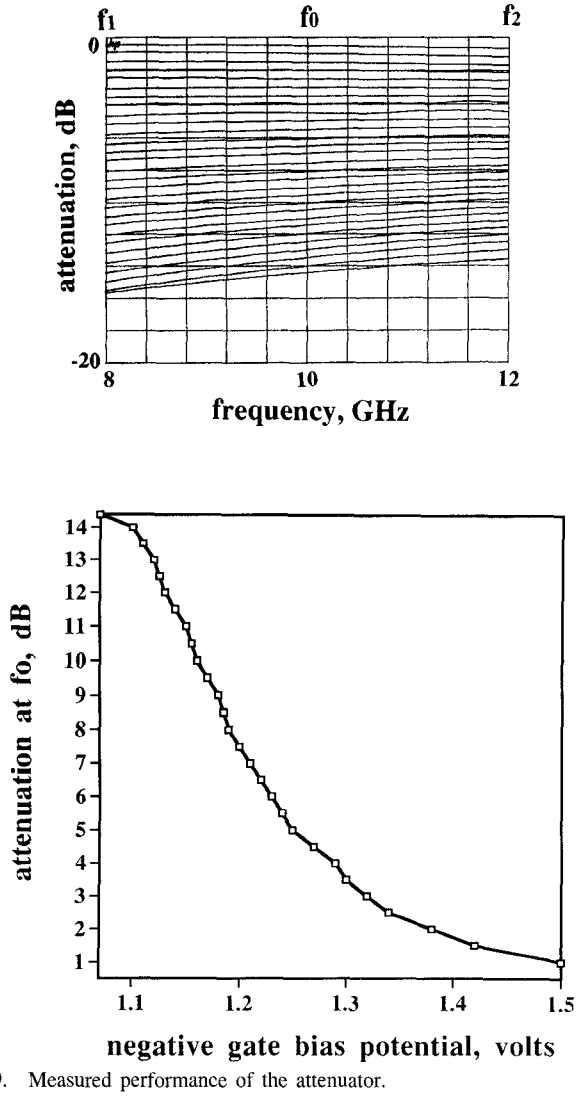

Fig. 9. Measured performance of the attenuator.

bandwidth covering 8 to 12 GHz. Hybrid technology has been used to realize an L-band group delay synthesizer operating with a center frequency of 1 GHz. With all the control devices, traditional microstrip techniques are used, employing folded 4-finger Lange couplers. The variable reactances are implemented with varactor diodes and the variable resistors are realized using cold-FET's. High value bias resistors are used to prevent RF leakage and as forward bias current limiters.

The GaAs MMIC's were fabricated at the GEC-Marconi (Caswell) foundry, using their standard low-cost F20 foundry process. A microphotograph for the phase shifter, delay line and attenuator are shown in Fig. 6(a). Standard 0.5 μm MESFET's are used to realize the variable capacitors [6], [7] and variable resistors. With the phase shifter and delay line, a back-to-back arrangement is adopted for the IPSVD's. This increases the maximum RF power level of the devices and reduces the errors in the resulting relative phase shift levels when operating at higher RF power levels [4]. The X-band MMIC control devices have an active area of 2.4 $\times$ 1.0 mm^2.

A photograph of the experimental hybrid MIC group delay synthesizer is shown in Fig. 6(b). Surface mounted bias resistors and DC blocking capacitors were attached directly onto the alumina substrate. The combined inductance of the bond wires, which connect the capacitors and cold-FET's together, form the reflection termination inductor. The complete L-band hybrid MIC group delay synthesizer has a total area of 1.0 $\times$ 1.0 in.^{2}.

IV. Measured Results

With the phase shifter operating in the *maximum relative phase shift* condition, the measured relative phase shift performance, with its associated tuning characteristic, are shown in Fig. 7(a). As expected, the rms phase error increases almost linearly from zero at center frequency to $\pm 2.5^\circ$ at the band edges. The corresponding group delay performance, with its associated variation in group delay, are shown in Fig. 7(b). The calculated variation in group delay has also been superimposed onto the measured results—demonstrating an almost perfect agreement. The mean level of insertion loss is 1.5 dB, with an rms amplitude error of ± 0.7 dB maintained at all levels of relative phase shift and at all frequencies. The worst-case return loss decreases almost linearly from 33 dB at center frequency to 18 dB at the band edges.

The measured relative phase shift performance, with its associated tuning characteristic, for the delay line are shown in Fig. 8(a). The corresponding group delay performance, with its associated variation in group delay, are shown in Fig. 8(b). The calculated variation in group delay for an ideal variable delay line has been superimposed onto the measured results—again, an almost perfect agreement is demonstrated. The variation in group delay for the phase shifter operating in the *minimum group delay variation* condition has also been included for comparison. The mean level of insertion loss is 1.6 dB, with an rms amplitude error of ± 0.6 dB maintained at all levels of relative phase shift and at all frequencies. The worst-case return loss decreases almost linearly from 28 dB at center frequency to 18 dB at the band edges.

For the variable attenuator, the measured levels of attenuation, with its associated tuning characteristic, are shown in Fig. 9. It can be seen that a good performance is found across a wide bandwidth. A dynamic range of 14 dB is achieved at center frequency. The worst-case return loss decreases almost linearly from 24 dB at center frequency to 19 dB at the band edges.

As with the other control devices, conventional on-wafer probing techniques were used to measure the hybrid MIC group delay synthesizer [15]. To facilitate this, a special grounded coplanar waveguide-to-microstrip transition was required [16]. The measured group delay performance, with its associated tuning characteristic, are shown in Fig. 10(a). As the negative gate bias potential increases from zero towards -2.43 V, the drain-source resistance increases towards $R_T = Zo^-$ and, therefore, the group delay approaches the positive singularity. Similarly, when the negative gate bias decreases from the punch-through potential towards -2.43 V, the drain-source resistance decreases towards $R_T = Zo^+$ and, therefore, the group delay approaches the negative singularity. The corresponding insertion loss performances, with its associated variation at center frequency, are shown in Fig. 10(b). One of

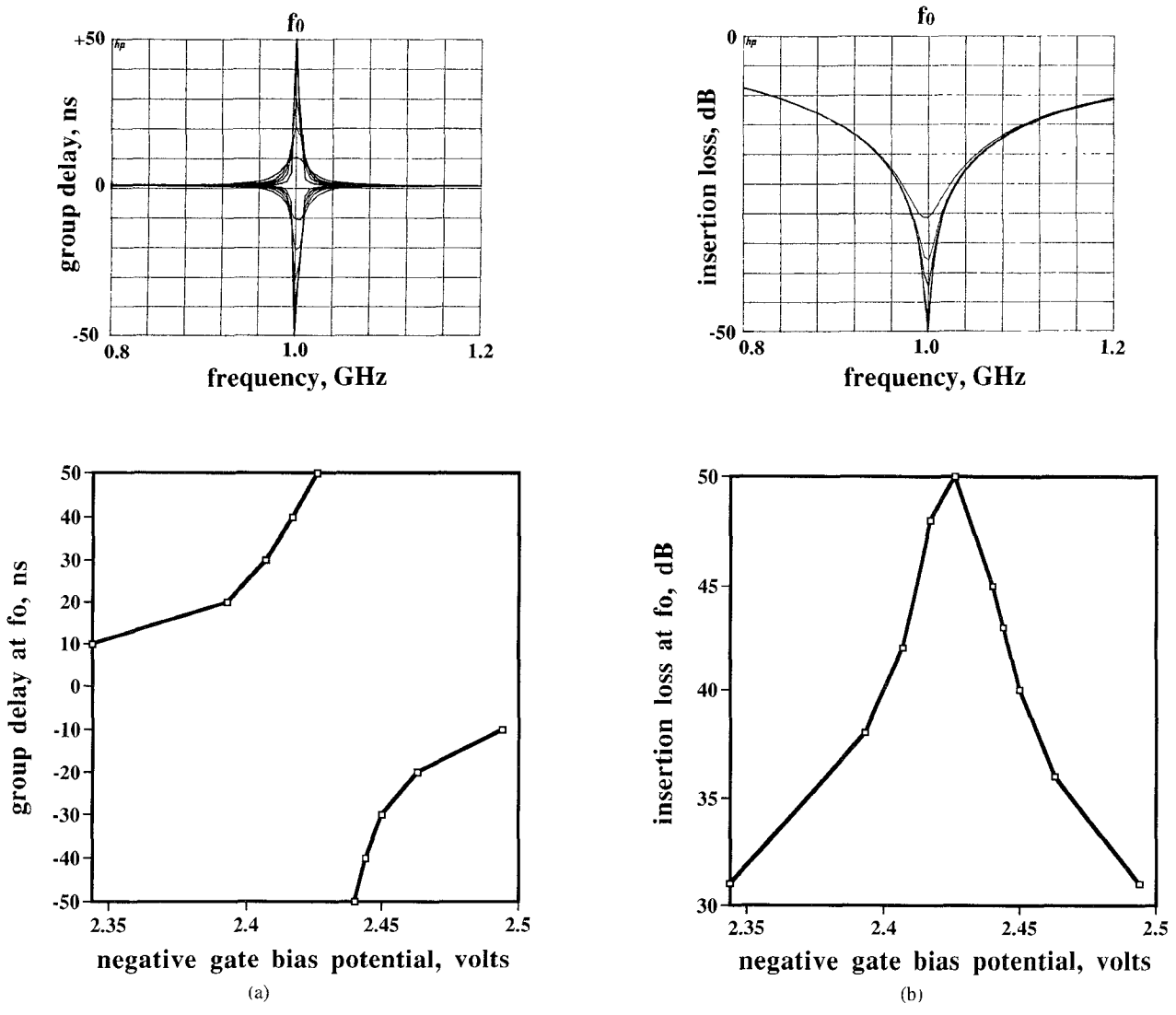

Fig. 10. Measured performance of the group delay synthesizer: (a) group delay; (b) insertion loss.

the inherent advantages with this synthesizer is its excellent return loss performance. The worst-case measured return loss was 26 dB. This enables the synthesizer to be embedded between two high gain amplifiers, required to overcome the high levels of insertion loss, without increasing the risk of instability.

V. Conclusion

A group of four individual analog control devices, which all share the same generic reflection topology, have been presented. The conditions required to achieve the optimal bandwidth performance for a variable phase shifter and variable delay line have been investigated in detail and demonstrated in practice.

Group delay is very sensitive to very small perturbations in the insertion phase frequency response. With a real directional coupler there is a significant deviation in the insertion phase frequency response from that of the ideal linear response, because of the finite isolation and return loss characteristics of a real coupler. When the effects of ideal feed lines to the coupler are taken into account, it becomes apparent that (12) is only a rough approximation. In practice, the measured values of absolute group delay at center frequency are lower that predicted by approximately 20%. However, the measured variations in group delay at center frequency are very close to those predicted using the equations presented here. Also, because of the non-idealities of the Lange coupler, the measured fractional bandwidths of the phase shifter are approximately double those predicted.

The high measured performance levels of the MMIC control devices make them ideal for use in: large adaptive beam forming networks; direct implementation transversal/recursive filters; and general microwave signal processing applications.

The group delay synthesizer could find applications in adaptive group delay equalization networks and even band stop filters. Also, when group delay is near a singularity it can be used to realize a non-drifting feedback oscillator. The oscillator could exhibit a high long-term stability, due to the very steep insertion phase gradients that can be achieved. These applications are totally compatible with MMIC technology–the

latter two offer the additional advantage of not requiring off-chip high-Q resonators. However, the noise performances would be rather poor, because of the high levels of insertion loss.

REFERENCES

[1] S. Lucyszyn and I. D. Robertson, "Decade bandwidth MMIC analogue phase shifter," *IEE Colloquium Dig. Multi-octave Microwave Circuits*, London, pp. 2/1-6, Nov. 1991

[2] ——, "Synthesis techniques for high performance octave bandwidth 180° analog phase shifters," *IEEE Trans. Microwave Theory Tech.*, vol. MTT-40, no. 4, pp. 731–739, Apr. 1992.

[3] R. N. Hardin, E. J. Downey, and J. Munushian, "Electronically–variable phase shifters utilizing variable capacitance diodes," *Proc. IRE*, vol. 48, pp. 944–945, May 1960.

[4] D. E. Dawson, A. L. Conti, S. H. Lee, G. F. Shade, and L. E. Dickens, "An analog X-band phase shifter," in *IEEE Microwave and Millimeter-Wave Monolithic Circuits Symp. Dig.*, 1984, pp. 6–10.

[5] G. E. Brehm, B. N. Scott, D. J. Seymour, W. R. Frensley, W. N. Duncan, and F. H. Doerbeck, "High capacitance ratio monolithic varactor diode," in *Cornell Microwave Conf.*, 1981, pp. 53–63.

[6] S. Lucyszyn, G. Green, and I. D. Robertson, "Accurate millimeter-wave large signal modeling of planar Schottky varactor diodes," in *IEEE MTT-S Int. Symp. Dig.*, 1992, pp. 259–262.

[7] ——, "Interdigitated planar Schottky varactor diodes for tunable MMIC applications," in *IEEE/ESA European Gallium Arsenide Applications Symp. Dig.*, ESTEC, Noordwijk, Apr. 1992.

[8] E. M. Bastida, G. P. Donzelli, and L. Scopelliti, "GaAs monolithic microwave integrated circuits using broadband tunable active inductors," in *Proc. 19th European Microwave Conf.*, 1989, pp. 1282–1287.

[9] S. Lucyszyn and I. D. Robertson, "Monolithic narrow band filter using ultra high-Q tunable active inductors," *IEEE Trans. Microwave Theory Tech.*, vol. MTT-42, no. 12, pp. 2617–2622, Dec. 1994.

[10] E. M. Rutz and J. E. Dye, "Frequency translation by phase modulation," *IRE WESCON Conv. Rec.*, pt. 1, pp. 201–207, 1957.

[11] H. N. Dawirs and W. G. Swarner, "A very fast, voltage controlled, microwave phase shifter," *Microwave J.*, pp. 99–107, June 1962.

[12] K. Wilson, J. M. C. Nicholas, G. McDermott, and J. W. Burns, "A novel MMIC X-band phase shifter," *IEEE Trans. Microwave Theory Tech.*, vol. MTT-33, no. 12, pp. 1572–1578, Dec. 1985.

[13] S. Lucyszyn, I. D. Robertson, and A. H. Aghvami, "High performance wideband analogue time shifter," *IEE Electron. Lett.*, vol. 29, no. 10, pp. 885–887, May 1993.

[14] L. M. Devlin and B. J. Minnis, "A versatile vector modulator design for MMIC," in *IEEE MTT-S Int. Symp. Dig.*, 1990, pp. 519–522.

[15] S. Lucyszyn, C. Stewart, I. D. Robertson, and A. H. Aghvami, "Measurement techniques for monolithic microwave integrated circuits," *IEE Electron. & Commun. Eng. J.*, pp. 69–76, Apr. 1994.

[16] S. Lucyszyn, I. D. Robertson, and A. H. Aghvami, "GCPW-to-microstrip transitions for measuring hybrid MICs using MMIC probing techniques," in *NPL 6th British Electromag. Meas. Conf. Dig.*, Teddington, UK, Nov. 1993, pp. 31/1-3.

Stepan Lucyszyn (M'91) was born in Bradford, England, in 1965. He received the Bachelors degree in electronic and communication engineering from the Polytechnic of North London in 1987. He then went on to gain a Masters degree in Satellite Communication Engineering from the University of Surrey, in 1988. This was followed by a year in the British and French space industries, working as a junior consultant on a broad range of projects. In 1992, he received the Ph.D. in electronic engineering from the University of London.

For the past three years, he has been undertaking research in the area of advanced microwave analog signal processing at King's College London. He has published over 35 technical papers in the area of microwave engineering in national and international conferences and journals.

Ian D. Robertson (M'91) was born in London, England, in 1963. He received the B.Sc. and Ph.D. degrees from King's College, University of London, in 1984 and 1990, respectively.

From 1984 to 1986 he was employed at Plessey Research (Caswell) in the MMIC Research Group, where he worked on MMIC mixers, on-wafer measurement techniques, and FET characterization. In 1986 he returned to King's as a research assistant, working on the T-SAT mobile communications payload. He is currently a lecturer at King's College and leader of the MMIC Research Team in the Communications Research Group. He has co-authored over 100 technical papers.